

# Computer-simulation calculations of the electronic stopping of slow, heavy charges by a classical harmonic oscillator

E. R. Custidiano,\* F. J. Pérez de la Rosa, and M. M. Jakas†

*Departamento de Física Fundamental y Experimental, Universidad de La Laguna, 38201 La Laguna, Tenerife, Spain*

(Received 26 June 2002; published 26 November 2002)

The interaction between slow, heavy pointlike charges and a classical electron harmonically bound to a heavy nucleus was studied by means of computer simulations. It is found that the equation of motion governing the interaction between a charge and classical harmonic oscillator can be conveniently scaled up so that the number of independent parameters is significantly reduced. Therefore, the stopping cross section  $S$  appears to be a universal function of Bohr's  $\xi$  parameter, the sign of the ion charge, and, with less significance, the scaled initial amplitude of the harmonic oscillator. Strikingly however, the stopping cross section of positive charges appears to be larger than that of negative ions at the same  $\xi$ . Moreover,  $S$  is found to be a linear function of the ion velocity for positive ions, whereas it is a nearly quadratic function for negative charges. It turns out that the mechanism responsible for the energy loss of positive ions is completely different from that of negative charges and, in both cases, different from those assumed in previous models of stopping of low-energy ions.

DOI: 10.1103/PhysRevA.66.052902

PACS number(s): 34.50.Bw, 79.20.Rf, 52.40.Mj, 61.85.+p

## I. INTRODUCTION

In order to calculate the electronic stopping of fast, heavy charges by solid matter, Bohr [1] replaced atoms by the ubiquitous classical harmonic oscillator (CHO). Since then, the CHO model has become widely used in dealing with the interaction of fast ions with solids, and this remains so even though more accurate quantum calculations have been published (see Refs. [2] and [3] and references therein). It is needless to say that the success of the CHO model is attributed to the fact that it is simple and yet fairly rich in terms of the number of processes it accounts for [4–6]. In addition, Bohr's CHO calculations were proven to be fairly accurate at high ion velocities.

The motion of a classical electron bound to a harmonic force and subjected to the Coulomb attraction of a moving charge constitutes a fairly complex problem. Actually, since it does not have exact analytical solutions, Bohr had to recourse to several approximations. The most important among these is the concept of *close* and *distant* collisions. These approximations allowed Bohr to calculate the mean energy loss as a function of the impact parameter in a simple, straightforward manner. However, while the *distant* collisions approximation poses no difficulties, in solving the close collisions Bohr neglected the harmonic forces and assumed that the ion-electron interaction is described by the Rutherford scattering law. By doing this, however, the stopping cross section so obtained is limited to cases of high ion velocities. At the time Bohr published his paper, this was not a serious drawback because most experiments were, then, performed using high-velocity ions from radioactive decay. Later on, however, interest shifted to lower energies, where

both theory and experiment have found significant difficulties.

It was not until recently, however, that Sigmund [4] managed to extend Bohr's stopping theory down to low velocities. But the results in Ref. [4] are based on an *ad hoc* procedure devised to interpolate between the close and distant collision approximations, rather than on physical arguments. Therefore, one cannot regard them as a rigorous extension of Bohr's CHO model to low bombarding energies. Motivated by this, we decided to carry out numerical simulations of the interaction between a pointlike charge and a classical electron harmonically bound to a heavy, positively charged nucleus. The results show that the CHO responds to a slowly moving charge in quite an interesting manner. Furthermore, the scaling law in Refs. [1,4] appears to be a feature of the combined Coulomb-harmonic potential itself and is not linked to any of the approximations introduced by Bohr in his calculations. A neat asymmetry appears between positive and negative charged ions. This low-velocity extension of the so-called Barkas effect (see Ref. [7] and references therein) suggests that the underlying mechanisms of the stopping strongly depend on the sign of the ion charge. A more detailed study, aimed at clarifying the origin of this asymmetry, shows that positive ions may literally trap the electron within the Coulomb potential for some time during the passage of the ion, a result that may have important implications for the assumption, commonly employed in stopping theories, that the electron absorbs energy in a single-scattering event.

It must be mentioned that no comparisons of our results with experimental data are produced in this paper. This stems from the fact that, to do so, it would imply deviating from our objective of studying the CHO model in the low-energy regime just "as is," i.e., with no additional assumptions and no approximations of any sort. In the following section the main assumptions utilized in these calculations are presented. The results of our simulations are shown in Sec. III together with a discussion of the most important consequences of our findings in this paper. Finally, a brief summary is offered in Sec. IV.

\*Permanent address: Departamento de Física, Facultad de Ciencias Exactas, Naturales y Agrimensura, Universidad Nacional del Nordeste, Avenida Libertad 5400, 3400-Corrientes, Argentina.

†Corresponding author. Email address: mmateo@ull.es

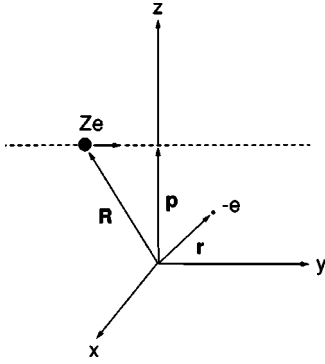


FIG. 1. Classical electron harmonically bound to a nucleus and exposed to the Coulomb attraction of a heavy ion.

## II. CALCULATIONS

In this paper we assume that a heavy, pointlike charged particle approaches from  $y = -\infty$  along a straight trajectory with impact parameter  $p$  and constant velocity  $v_0$ . At the origin of the frame of reference a heavy nucleus holds a classical electron through a harmonic force (see Fig. 1). Therefore, the equation governing the motion of the electron can be written as

$$m \frac{d^2 \mathbf{r}}{dt^2} = -m\omega^2 \mathbf{r} - Ze^2 \frac{\mathbf{r} - \mathbf{R}}{|\mathbf{r} - \mathbf{R}|^3}, \quad (1)$$

where  $\mathbf{R} = \mathbf{k}_z p + \mathbf{k}_y v_0 t$  and

$$\mathbf{r}(t) = A(\mathbf{n}_1 \cos \omega t + \mathbf{n}_2 \sin \omega t) \quad \text{for } t \rightarrow -\infty, \quad (2)$$

where  $Z$  is the number charge of the projectile,  $e$  is the unit charge,  $\omega$  is the frequency of the harmonic potential,  $m$  is the electron mass and,  $\mathbf{k}_y$  and  $\mathbf{k}_z$  denote unit vectors along  $y$  and  $z$  directions, respectively. Similarly,  $A$  is the amplitude of the oscillation, and  $\mathbf{n}_1$  and  $\mathbf{n}_2$  are three-dimensional vectors which are subject to the equation  $\mathbf{n}_1^2 + \mathbf{n}_2^2 = 1$ .

It can be readily verified that if one replaces  $\mathbf{r}$  and  $t$  by the dimensionless variables  $\boldsymbol{\rho}$  and  $\tau$ , where  $\boldsymbol{\rho} = \mathbf{r}\omega/v_0$  and  $\tau = t\omega$ , then Eq. (1) can be rewritten as

$$\frac{d^2 \boldsymbol{\rho}}{d\tau^2} = -\boldsymbol{\rho} - \left(\frac{1}{\xi}\right) \frac{\boldsymbol{\rho} - \mathbf{P}}{|\boldsymbol{\rho} - \mathbf{P}|^3}, \quad (3)$$

$\mathbf{P} = \mathbf{k}_z b + \mathbf{k}_y \tau$ , and

$$\boldsymbol{\rho}(t) = a(\mathbf{n}_1 \cos \tau + \mathbf{n}_2 \sin \tau) \quad \text{for } \tau \rightarrow -\infty, \quad (4)$$

where  $\xi = mv_0^3/Ze^2\omega$ ,  $b = p\omega/v_0$ , and  $a = A\omega/v_0$ .

It must be noticed that by using the scaling above one reduces the number of independent parameters from five, namely,  $Z$ ,  $\omega$ ,  $v_0$ ,  $A$ , and  $p$ , to three:  $a$ ,  $\xi$ , and  $b$ . As a consequence, the energy transferred to the electron previously divided by the unit of energy, namely,  $mv_0^2$ , must be a function of  $a$ ,  $\xi$ , and  $b$  and, similarly, the scaled stopping cross section  $\bar{\mathcal{S}}$  must be a *sole* function of  $a$  and  $\xi$ , i.e.,

$$2\pi \int \bar{\Delta \varepsilon} b db = \bar{\mathcal{S}}(a, \xi), \quad (5)$$

where  $\bar{\Delta \varepsilon}$  denotes the mean energy loss value, in reduced units, averaged over a distribution of initial conditions.

In order to obtain  $\Delta \varepsilon$  a computer program was developed which simulates the motion of the electron during the passage of the ion. Our approach is similar to that used in Ref. [8] to study the ionization of hydrogen by fast ions. Here, Eq. (3) is solved by means of a standard four-point Runge-Kutta scheme with an adaptive time step as described in Ref. [9]. As initial conditions, we place the projectile to the left of a distance from the nucleus so that the potential energy of the electron in the field of the ion is negligible. Similarly, the position and velocity of the electron are assumed to be isotropically distributed, with the condition that the spatial amplitude of the oscillations is fixed and equal to  $\alpha$ . Finally, the integration is stopped when the projectile is far away to the right of the nucleus and the ion-electron potential has dropped below the same value as that used before the collision. Finally, the energy loss for a particular ion trajectory is obtained by subtracting the final and the initial energy of the electron for such a trajectory, i.e.,

$$\Delta \varepsilon_j = \varepsilon_j^{(f)} - \varepsilon_j^{(i)}, \quad (6)$$

where  $\varepsilon_j^{(i(f))}$  stands for the total initial (final) energy of the electron in the  $j$ th trajectory. In connection with this, it must be mentioned that the numerical program verifies that the difference between the final and initial potential energy of the electron in the field of the ion is negligible and that it has no significant effects on the energy-loss calculations.

After simulating  $N$  statistically independent trajectories we can calculate the mean energy loss for a given impact parameter as in

$$\bar{\Delta \varepsilon} = \frac{1}{N} \sum_{j=1, \dots, N} \Delta \varepsilon_j, \quad (7)$$

where  $N$  is determined by the statistical significance requested for  $\bar{\Delta \varepsilon}$ . In this regard, it must be mentioned that most results in this paper have a relative error of 10%, or less. Therefore, depending on the case,  $N$  may run from few hundreds up to several thousands trajectories. Similarly, the whole process can be repeated for a set of impact parameters and so, the stopping cross section is obtained as indicated in Eq. (5).

## III. RESULTS AND DISCUSSION

In this section we present the results of calculating the stopping cross section  $\bar{\mathcal{S}}$  according to the numerical procedure described in the preceding section. In Fig. 2 we plot  $\bar{\mathcal{S}}$  as a function of  $\xi$  for positive and negative charged ions, and the electron in the harmonic oscillator with no initial energy, i.e.,  $a=0$ . It must be noted though that in this section  $\xi$  will be assumed to be a positive number, with the sign of the ion charge [ $\text{sgn}(Z)$ ] as an independent parameter.

In the first place, the results in Fig. 2 show that the sign of the ion charge appears to be an important parameter here. In fact, one can readily see that, depending on the sign of  $Z$ , the stopping cross sections can be grouped into two different

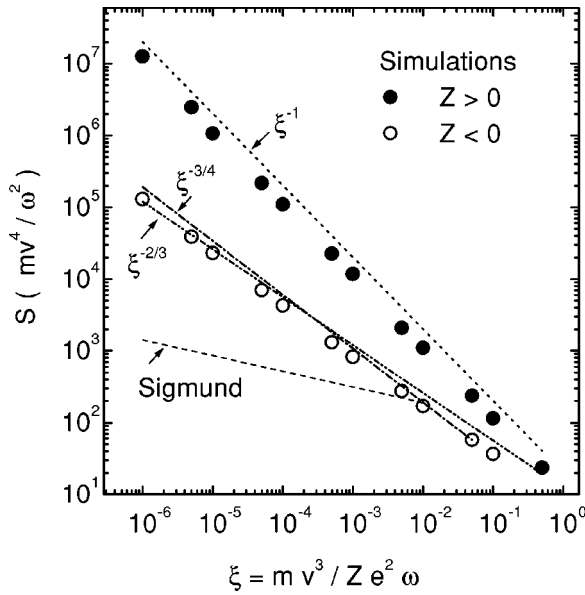


FIG. 2. Stopping cross section as a function of  $|\xi|$ . Results of simulations appear as symbols: ● for positive and ○ for negative ions, respectively. In both cases, the amplitude of the harmonic oscillator is  $a=0$ . Theoretical results in Ref. [4] appear as a dashed curve. To compare the slope of simulations, functions  $\xi^{-1}$  (dotted),  $\xi^{-3/4}$  (dot-dashed), and  $\xi^{-2/3}$  (double-dot-dashed) are plotted in the same figure.

curves. Notably enough, that of positive ions appears to be proportional to  $\xi^{-1}$  whereas that of the negative ions lies below the former and exhibits a smaller slope, i.e.,  $S \propto \xi^{-\nu}$  with  $\nu$  between  $\frac{2}{3}$  and  $\frac{3}{4}$ . It must be stressed, however, that the fact that for positive charges  $S$  is proportional to  $\xi^{-1}$  implies that the stopping cross section  $S$ , in normal units, is a linear function of the ion velocity, i.e.,  $S \propto v_0$ , whereas for negative ions one has  $S \propto v_0^{1.75-2}$ . In both cases, however, and this must be remarked, the present simulations do not agree with the predictions in Ref. [4].

Figure 3 shows that giving the electron an initial amplitude  $a=10$  leads to smaller stopping cross sections. Furthermore, the reduction seems to be larger, the greater the  $\xi$ ; and observe that positive charges seem to be more sensitive to such an increase than negative ions. Actually, in the case of negative charges one has to go to a  $\xi$  as large as  $10^{-3}$  to see a significant difference between the results of  $a=10$  and those of  $a=0$ , whereas for positive ions the two curves are already separated at  $\xi=10^{-5}$ . The fact that the stopping becomes less sensitive to  $a$  with a decrease of  $\xi$  can be readily explained using the scaled equation of motion derived in the preceding section. In fact, Eq. (3) shows that a decrease of  $\xi$  leads to a stronger “reduced” Coulomb potential, and therefore, by reducing  $\xi$  while keeping  $a$  fixed, one is reducing the electron’s initial energy compared to the interaction energy. One can conceivably expect, therefore, that with a decrease of  $\xi$ , the electron motion, and so the stopping, becomes less dependent on  $a$ . With regard to the different degrees of sensitivity exhibited by positive and negative ions against changes of  $a$ , we can offer no explanation other than saying that it seems to be linked to the difference that appears to

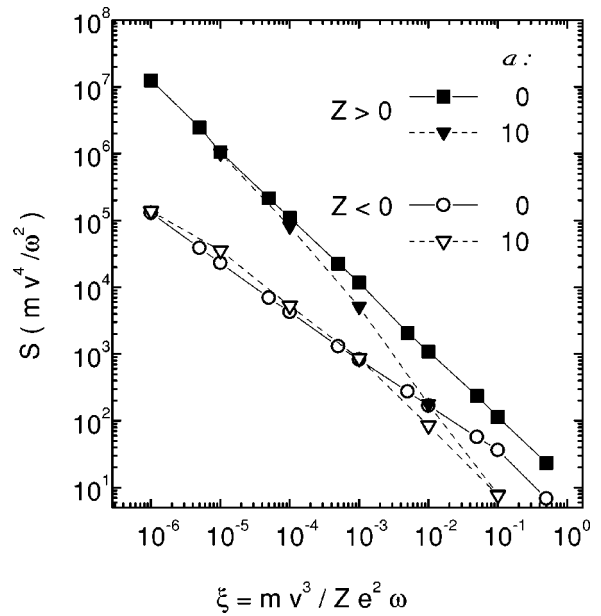


FIG. 3. Stopping cross section as a function of  $|\xi|$  for positively (solid symbols) and negatively (open symbols) charged ions, and initial amplitude of the harmonic oscillator  $a=0$  (squares) and  $10$  (down triangles).

exist between the mechanism responsible for the energy loss of positive and negative charges.

In order to understand the results in Fig. 2 we shall carry out order-of-magnitude estimates of the mean energy loss for positive and negatively charged particles and for the limiting cases of low bombarding velocities. To begin with, let us consider a negatively charged projectile. In this case, as the ion approaches the harmonic oscillator, the electron is repelled and pushed away from the ion path (see Fig. 4). Therefore, one can conceivably assume that the electron is never exposed to the strong core of the Coulomb potential as in the case of a positive charge. This suggests that Bohr’s

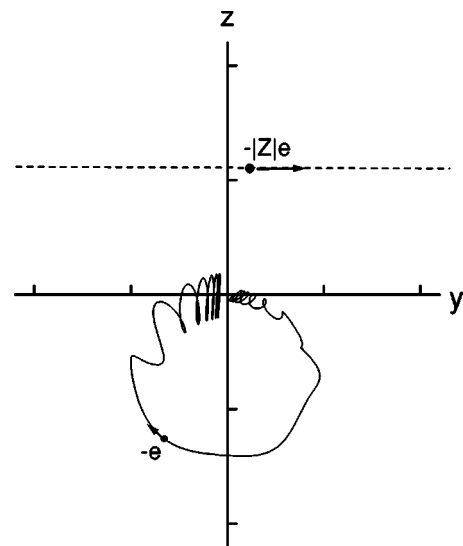


FIG. 4. Trajectory of the electron during the passage of a negatively charged ion with impact parameter  $b=0.5$  and  $|\xi|=10^{-3}$ .

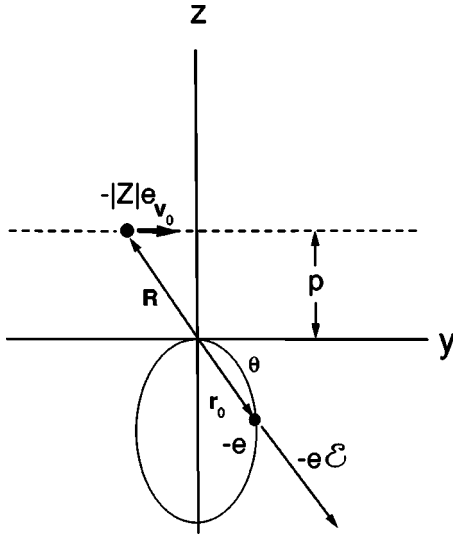


FIG. 5. Equilibrium or zero-force position of the electron in the harmonic oscillator  $\mathbf{r}_0$  under the repulsive force of a negatively charged ion located at  $\mathbf{R}$ .

concept of distant collision might hold though; in order to use the same procedure as that of Bohr's, some additional assumptions must be made.

In the first place, one may assume that the electron is, all the time, oscillating around the point where the net force is zero, i.e.,  $\rho_0$ . This "zero-force" position can be readily calculated using Eq. (3), i.e.,

$$\rho_0 = -\left(\frac{1}{\xi}\right) \frac{\rho_0 - \mathbf{P}}{|\rho_0 - \mathbf{P}|^3}, \quad (8)$$

where, as was previously defined,  $\mathbf{P} = \mathbf{k}_z b + \mathbf{k}_y \tau$ .

Furthermore, one can reasonably assume that  $\rho_0 = \mathbf{r}_0 \omega / v_0$  will be parallel to  $\mathbf{P} = \mathbf{R} \omega / v_0$ , though with opposite direction (see Fig. 5). Therefore, we can disregard the vector nature of  $\rho_0$  and  $\mathbf{P}$ , and work with them as if they were scalar variables, i.e.,  $\rho_0$  and  $P$ . In consequence, assuming that  $P$  is positive,  $\rho_0$  can be obtained as the real root of the cubic equation,

$$\rho_0(\rho_0 - P)^2 + \frac{1}{\xi} = 0, \quad (9)$$

which can be conveniently scaled up using  $\tilde{\rho}_0 = \rho_0 \xi^{1/3}$  and  $\tilde{P} = P \xi^{1/3}$ , thus the dependence with  $\xi$  is removed and we obtain the equation

$$\tilde{\rho}_0(\tilde{\rho}_0 - \tilde{P})^2 + 1 = 0, \quad (10)$$

which be readily solved, the result being [10]

$$\tilde{\rho}_0 = s_1 + s_2 + \frac{2}{3}, \quad (11)$$

where

$$s_1 = -\left[\left(\frac{\tilde{P}}{3}\right)^3 + \frac{1}{2} + \sqrt{\frac{1}{4} + \left(\frac{\tilde{P}}{3}\right)^3}\right]^{1/3},$$

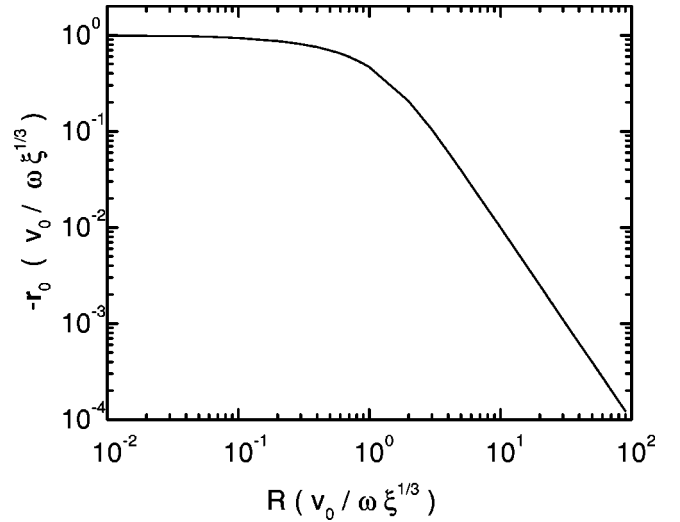


FIG. 6. The zero-force position,  $\rho_0 = r_0 \omega / v_0$ , for the electron as a function of the distance of the negatively charged ion  $P = R \omega / v_0$  measured with respect to the center of the harmonic potential [see Eqs. (8)–(12)].

$$s_2 = -\left[\left(\frac{\tilde{P}}{3}\right)^3 + \frac{1}{2} - \sqrt{\frac{1}{4} + \left(\frac{\tilde{P}}{3}\right)^3}\right]^{1/3}. \quad (12)$$

Using the expressions above one can easily verify that  $\tilde{\rho}_0 = -1$  for  $\tilde{P} = 0$ , and that  $\tilde{\rho}_0 \propto -\tilde{P}^{-2}$  with  $\tilde{P} \gg 1$  as shown in Fig. 6.

According to our previous arguments, we can use the dipolar approximation introduced by Bohr to obtain the mean energy loss in the distant collisions, i.e., [11],

$$\Delta E(p) = \frac{\pi}{e^2} |\tilde{\mathcal{E}}(\omega, p)|^2, \quad (13)$$

provided that the Fourier transform of the electric field due to the ion, i.e.,  $\tilde{\mathcal{E}}(\omega, p)$ , is not evaluated right at the center of the harmonic oscillator as Bohr did, but at the instantaneous oscillation center  $\mathbf{r}_0 = v_0 \rho_0 / \omega$  (see the Appendix). That is,

$$\tilde{\mathcal{E}}(\omega, p) = \frac{Ze}{\sqrt{2\pi}} \int_{-\infty}^{+\infty} dt \frac{\mathbf{r}_0 - \mathbf{R}}{|\mathbf{r}_0 - \mathbf{R}|^3} e^{-it\omega}, \quad (14)$$

which, using the previously introduced dimensionless variables, reduces to

$$\tilde{\mathcal{E}}(\omega, b) = \frac{Ze\omega}{\sqrt{2\pi}v_0^2} \int_{-\infty}^{+\infty} d\tau \frac{\rho_0 - \mathbf{P}}{|\rho_0 - \mathbf{P}|^3} e^{-i\tau}, \quad (15)$$

and according to the frame of reference shown in Fig. 5 and the parity of the integrands, we thus have

$$\tilde{\mathcal{E}}(\omega, b) = \frac{Ze\omega}{\sqrt{2\pi}v_0^2} \times \int_{-\infty}^{+\infty} d\tau \frac{\mathbf{k}_z \cos \theta \cos \tau - \mathbf{k}_y i \tau \sin \theta \sin \tau}{(\rho_0 - P)^2}, \quad (16)$$

where  $\cos \theta = \tau/P$  and  $\sin \theta = b/P$ .

For small  $\xi$  values, however, not only  $\rho_0$  is a fairly slowly varying function of  $\tau$ , but also  $\rho_0 \gg P$  for a considerably large range of  $\tau$  around  $\tau=0$ . In that case,  $(\rho_0 - P)^2$  can be taken out of the integration and replaced by  $(\xi^{-1/3} + b)^2$ , thus Eq. (16) can be written as

$$\tilde{\mathcal{E}}(\omega, p) \approx \frac{Ze\omega}{\sqrt{2\pi v_0^2}(\xi^{-1/3} + b)^2} \mathbf{g}(b), \quad (17)$$

where

$$\begin{aligned} \mathbf{g}(b) &= \int_{-\infty}^{+\infty} d\tau (\mathbf{k}_x \cos \theta \cos \tau - \mathbf{k}_y i \tau \sin \theta \sin \tau) \\ &= 2b[\mathbf{k}_z K_1(b) - \mathbf{k}_y i K_0(b)], \end{aligned} \quad (18)$$

where  $K_0$  and  $K_1$  are the modified Bessel function of first and second order, respectively [10].

Since both  $K_0(b)$  and  $K_1(b)$  drop to zero faster than  $(\xi^{-1/3} + b)^{-2}$ , we can write

$$\tilde{\mathcal{E}}(\omega, b) \approx \frac{Ze\omega \xi^{2/3}}{\sqrt{2\pi v_0^2}} \mathbf{g}(b) \quad (19)$$

and

$$\Delta E(p) \approx \frac{Z^2 e^4 \xi^{4/3} \omega^2}{2m v_0^4} |\mathbf{g}|^2 (p\omega/v_0) = \frac{m v_0^2}{2\xi^{2/3}} |\mathbf{g}|^2 (p\omega/v_0). \quad (20)$$

Finally, the stopping cross section becomes

$$S \approx 4\pi \frac{m v_0^4}{\omega^2 \xi^{2/3}}, \quad (21)$$

or

$$\tilde{S} = S\omega^2/(m v_0^4) = 4\pi \xi^{-2/3}, \quad (22)$$

a result that agrees fairly well with simulations (see Fig. 9).

We now turn our attention to the case of positively charged ions. The fact that the Coulomb potential is now attractive makes the situation completely different. During the approaching stage, when the ion is far away from the harmonic oscillator, the harmonic potential prevents the electron from getting close to the ion. At some point, when the ion gets close enough to the center of the harmonic potential, the electron can be captured by the ion and, from that moment the electron remains orbiting around the ion until the process just described occurs in a reverse order: The ion releases the electron and it comes back to the harmonic potential.

Since the binding energy in the harmonic potential is infinite, the electron cannot be captured by the ion. Therefore, the word ‘‘capture’’ is used here in the sense of identifying the potential which dominates and, consequently, determining the electron’s motion. In connection with this, it is worth adding that our simulations show that, in the case of positive ions, the electron’s trajectories appear to be dominated by

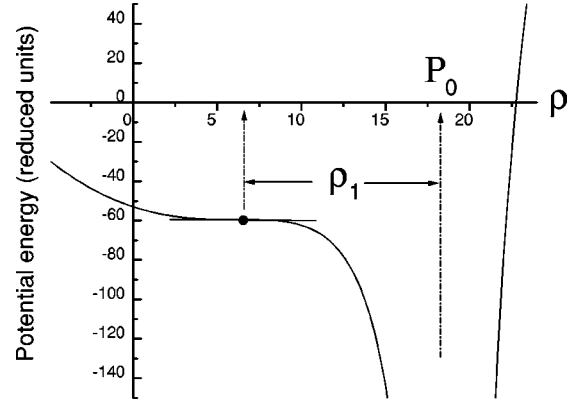


FIG. 7. Potential energy of the electron as a function of the position, in reduced units, at the critical distance of the ion for capturing the electron ( $P_0$ ).

only one potential at a time, that is, either by the harmonic or by the ion’s Coulomb potential, but not the two of them simultaneously. This should not be confused with what happens in Bohr’s close collisions where the Coulomb and the harmonic potentials can be thought of as acting separately because of the huge difference that exists between the time scaling of these two interactions.

To begin with, we shall calculate the distance at which the electron can be captured by the ion. To this end, one may conceivably assume that the ion is in a position of capturing the electron if no point exists along the straight line which connects the ion and the center of the harmonic potential, where the force is directed towards the latter. This obviously occurs when, along that line, the potential energy has an extreme which is also an inflexion point, i.e.,  $\rho_1$  in Fig. 7.

Using the previously introduced dimensionless variables, the distance of the ion at which capture may occur—measured from the center of the harmonic potential—becomes

$$P_0 = 3/(4\xi)^{1/3}. \quad (23)$$

Second, we assume that the ion captures the electron as soon as it is situated at the previously calculated distance from the origin, i.e.,  $P_0$ . From that moment, the electron is subjected to the strong, attractive field of the ion and starts orbiting around it. This remains so until the ion is found again at a distance  $P_0$  during the second half of the collision. Then the electron may escape from the Coulomb attraction of the ion and starts oscillating around the origin again. This last process however may take some additional time, since the electron may accompany the ion beyond the critical distance  $P_0$ . Obviously, such additional distance is determined by the time the electron may need to actually escape from the Coulomb attraction, namely,  $fT$ , where  $T$  is the period of the electron in the Coulombic trajectory, and  $f$  is a non-negative, less than unity number, indicating that it may take a fraction of the period  $T$ .

According to the previous, approximate description of the interaction between the positive charge and the harmonic oscillator, the energy is transferred to the electron as a result of the difference between distances up to which the electron is



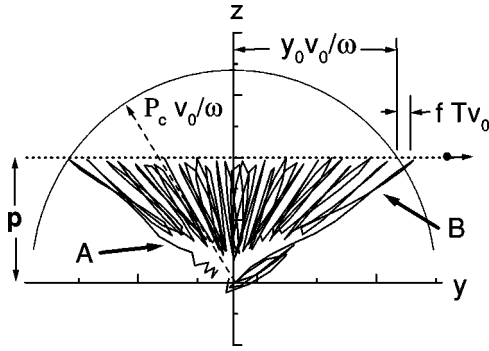


FIG. 8. Capture (A) and release (B) of the electron by the positively charged ion during the first and second halves of the collision, respectively. This trajectory is the result of simulating the passage of a positive ion with impact parameter  $b=1$  and  $|\xi|=10^{-3}$ .

taken at the time of release from the Coulomb field and capture into the Coulomb field, respectively. This is illustrated in Fig. 8 from where one can readily verify that

$$\Delta E(p) \approx \frac{1}{2} m v_0^2 [(y_0 + f T \omega)^2 - y_0^2], \quad (24)$$

where  $y_0 = \sqrt{P_0^2 - (p\omega/v_0)^2}$  and  $f T \omega$  accounts for the distance the ion moved during time  $f T$ , in reduced units.

In the first place, observe that within the approximation above, a maximum impact parameter does exist for which  $\Delta E(p) \neq 0$ , namely,  $p_{\max} = v_0 P_0 / \omega$ . Furthermore, since at low ion velocities  $y_0$  is generally much more larger than  $f T \omega$ , we may therefore write

$$\Delta E(p) \approx m v_0^2 y_0 f T \omega. \quad (25)$$

In order to proceed with our calculation we need an estimate for  $T$ . However, as is well known, for a Coulomb potential [12]  $T = 2\pi m^{1/2} Z e^2 / (2|E|)^{3/2}$ , where  $E$  is the total energy of the electron. The latter can be readily calculated by taking into account that for low ion velocities, the total energy is given by the potential energy the electron has right at the time of being captured by the ion, that is,  $-Z e^2 \omega / (v_0 \rho_1)$  (see Fig. 7). Since  $\rho_1 = 2/(4\xi)^{1/3}$  we thus obtain  $E = -(4mZ^2 e^4 \omega^2)^{1/3} / 2$  and  $T = \pi / \omega$ . By combining these results, we find

$$\Delta E(p) \approx \pi^2 f m v_0^2 \sqrt{P_0^2 - (p\omega/v_0)^2}, \quad (26)$$

which can be also written as

$$\Delta E(p) \approx \frac{3\pi f m v_0^2}{(4\xi)^{1/3}} \sqrt{1 - [(4\xi)^{1/3} p \omega / (3v_0)]^2}. \quad (27)$$

From this equation, and taking into account that  $\Delta E(p) = 0$  for  $p > p_{\max}$ , one can readily obtain the stopping cross section. The result becomes

$$S = \frac{9\pi^2 f m v_0^4}{2 \omega^2 \xi} \approx 44f \frac{m v_0^4}{\omega^2 \xi}; \quad (28)$$

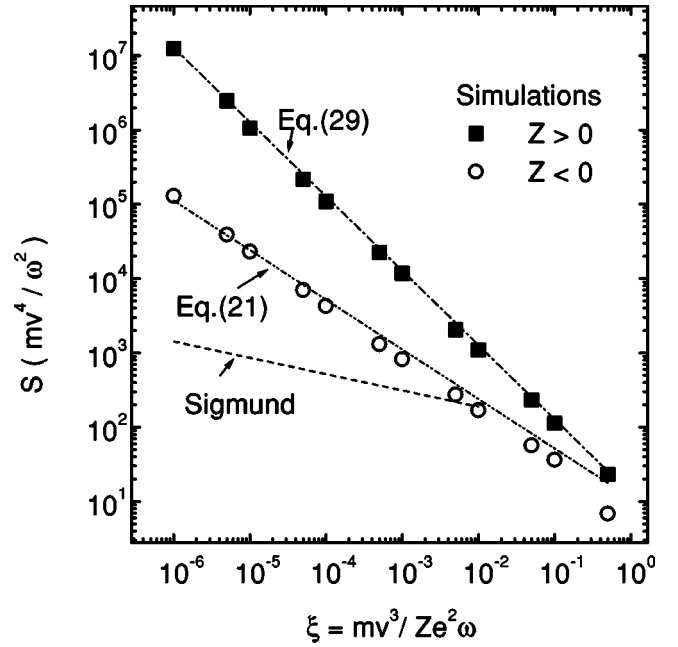


FIG. 9. Same as Fig. 2. Lines, however, stand for theoretical results in Eqs. (21) (dashed) and (29) (dotted).

alternatively, using our previously mentioned scaling, one has

$$\tilde{S} = S \omega^2 / (m v_0^4) = 44f / \xi, \quad (29)$$

a result that can be readily brought into coincidence with simulations if one chooses  $f \approx 1/4$ ; thus,  $\tilde{S} \approx 11/\xi$ .

We have plotted our “order-of-magnitude” estimates in Fig. 9 and one can readily see that our results, i.e., Eqs. (22) and (29), compare remarkably well with simulations. This tells us that the two approximate models above are even more accurate than one could have possibly imagined and, consequently, that the energy loss of slow ions stems from mechanisms that substantially differ from those of swifter ions.

#### IV. SUMMARY AND CONCLUDING REMARKS

With the purpose of extending Bohr’s stopping theory down to low-velocity ions, we have simulated the interaction between a slowly moving, heavy charge and a classical harmonic oscillator. The results in the present simulations can be summarized as follows.

(1) The stopping cross section  $S$  previously multiplied by  $\omega^2 / (m v_0^4)$  seems to be a *universal* function of  $\xi = m v_0^3 / (|Z| e^2 \omega)$ , the sign of the ion charge, i.e.,  $\text{sgn}(Z)$ , and, to a lesser degree, the initial amplitude of the electron motion in the harmonic oscillator.

(2) In the case of negatively charged ions, one can apply Bohr’s concept of *distant* collisions all the way down to small impact parameters. The difference, however, being that when using the dipolar approximation, the electric field of the ion should not be calculated right at the center of the

harmonic oscillator, as Bohr did, but along the “zero-force” position (see text).

(3) For positive ions things are totally different. Contrary to what is assumed in Ref. [4], the electron appears to undergo not just one but a series of scatterings with the incoming ion. Strikingly however, the energy loss does not seem to be caused by these multiple interactions, but mainly by the fact that the electron is literally captured by the ion and released in a high-energy state during the second half of the ion-CHO interaction.

Although the results in this paper are based on a classical harmonic oscillator and one cannot guarantee that they can be observed in a quantum oscillator or apply to other, more realistic potentials, the important role that multiple interactions appear to have, particularly in the case of positive ions, is remarkable. This warns us that single-scattering-based models may not accurately describe the stopping of low-velocity ions. Actually, a model such as that described in Ref. [13] appears to be more closely connected to our observations in this paper than those in earlier theoretical works on the stopping of low-energy ions [14].

#### ACKNOWLEDGMENTS

This work was supported in part by the Consejería de Educación, Cultura y Deportes of Gobierno Autónomo de Canarias (Spain). One of us (E.R.C.) wishes to thank the Secretaría de Ciencia y Técnica of the Universidad Nacional del Nordeste (Argentina) for the financial support that made possible his visit to the Universidad de La Laguna (Spain). We are indebted to T. A. Paporo for his valuable help during the preparation of this manuscript.

#### APPENDIX

##### Approximate solution for negative ions

Let us begin with the equation of motion (3) for the electron in the field of the harmonic oscillator and a negative projectile,

$$\frac{d^2 \boldsymbol{\rho}}{d\tau^2} = -\boldsymbol{\rho} + \left( \frac{1}{\xi} \right) \frac{\boldsymbol{\rho} - \mathbf{P}}{|\boldsymbol{\rho} - \mathbf{P}|^3}, \quad (\text{A1})$$

where  $\mathbf{P} = \mathbf{k}_z b + \mathbf{k}_y \tau$ .

We can expand the equation above around the zero-force position, i.e.,  $\boldsymbol{\rho}_0$ ; thus taking into account Eq. (8) one has

$$\frac{d^2(\boldsymbol{\rho}_0 + \boldsymbol{\delta})}{d\tau^2} = - \left( 1 - \frac{1/\xi}{|\boldsymbol{\rho}_0 - \mathbf{P}|^3} \right) \boldsymbol{\delta} - \left( \frac{3}{\xi} \right) \frac{\boldsymbol{\rho}_0 \cdot \boldsymbol{\delta}}{|\boldsymbol{\rho}_0 - \mathbf{P}|^5} (\boldsymbol{\rho}_0 - \mathbf{P}). \quad (\text{A2})$$

For an order-of-magnitude estimate, Eq. (A2) can be approximated as

$$\frac{d^2 \boldsymbol{\delta}}{d\tau^2} \approx -\boldsymbol{\delta} - \frac{d^2 \boldsymbol{\rho}_0}{d\tau^2}. \quad (\text{A3})$$

The solution of Eq. (A3) can be readily obtained, since it describes a unit mass and frequency harmonic oscillator with  $-d^2 \boldsymbol{\rho}_0 / d\tau^2$  as the external force. Therefore, assuming  $|\boldsymbol{\delta}| = 0$  as the initial condition, one has

$$\lim_{\tau \rightarrow +\infty} |\boldsymbol{\delta}| \approx \left| \int_{-\infty}^{+\infty} d\tau \frac{d^2 \boldsymbol{\rho}_0}{d\tau^2} e^{-i\tau} \right| = \left| \int_{-\infty}^{+\infty} d\tau \boldsymbol{\rho}_0 e^{-i\tau} \right|, \quad (\text{A4})$$

which can be alternatively written as

$$\lim_{\tau \rightarrow +\infty} |\boldsymbol{\delta}| = \left| \frac{1}{\xi} \int_{-\infty}^{+\infty} d\tau \frac{\boldsymbol{\rho}_0 - \mathbf{P}}{|\boldsymbol{\rho}_0 - \mathbf{P}|^3} e^{-i\tau} \right|, \quad (\text{A5})$$

thus proving that the solution of Eq. (A1) can be obtained using the dipolar approximation at the zero-force point in place of the center of the harmonic oscillator as utilized by Bohr in Ref. [1].

- 
- [1] N. Bohr, *Philos. Mag.* **25**, 10 (1913).  
 [2] U. Fano, *Ann. Nucl. Sci.* **13**, 1 (1963).  
 [3] P. M. Echenique, F. Flores, and R. H. Ritchie, *Solid State Phys.* **43**, 229 (1990).  
 [4] P. Sigmund, *Phys. Rev. A* **54**, 3113 (1996).  
 [5] P. Sigmund and A. Schinner, *Eur. Phys. J. D* **12**, 425 (2000).  
 [6] P. Sigmund, *Eur. Phys. J. D* **12**, 111 (2000).  
 [7] H. H. Mikkelsen and H. Flyvbjerg, *Phys. Rev. A* **45**, 3025 (1992).  
 [8] R. E. Olson and A. Salop, *Phys. Rev. A* **16**, 531 (1977); see also C. O. Reinhold and R. E. Olson, *ibid.* **39**, 3861 (1989).  
 [9] W. H. Press, B. P. Flannery, S. A. Teukolsky, and William T. Vetterling, in *Numerical Recipes. The Art of Scientific Computing* (Cambridge University Press, Cambridge, 1986).  
 [10] *Handbook of Mathematical Functions*, edited by M. Abramowitz and I. A. Stegun (Dover, New York, 1972).  
 [11] J. D. Jackson, *Classical Electrodynamics* (Wiley, New York, 1999), Chap. 13.  
 [12] D. Landau, L. P. Pitaevskii, and E. M. Lifshitz, *Mechanics*, (Butterworth-Heinemann, Oxford 1976), Vol. 1.  
 [13] M. Kato and R. Smith, *Nucl. Instrum. Methods Phys. Res. B* **153**, 36 (1999).  
 [14] E. Fermi and E. Teller, *Phys. Rev.* **72**, 399 (1947); O. B. Firsov, *Zh. Eksp. Teor. Fiz.* **36**, 1517 (1959) [*Sov. Phys. JETP* **36**, 1076 (1959)]; J. Lindhard and M. Scharff, *Phys. Rev.* **124**, 128 (1961).